Channeling of charge carrier plasmons in carbon nanotubes

C. Kramberger,[1] F. Roth,[2] R. Schuster,[2] R. Kraus,[2] M. Knupfer,[2]
E. Einarsson,[1] S. Maruyama,[1] D. Mowbray,[3] A. Rubio,[3,4] and T. Pichler[5]

[1] *University of Tokyo, Department of Mechanical Engineering, 7-3-1 Hongo, Bunkyo-ku, Tokyo 113-8656, Japan*
[2] *IFW Dresden, Helmholtzstraße 20, D-01069 Dresden, Germany*
[3] *Nano-bio Spectroscopy Group and ETSF Scientific Development Centre, Departamento de Física de Materiales, Universidad del País Vasco, Centro de Física de Materiales CSIC-UPV/EHU-MPC and DIPC, Avenida de Tolosa 72, E-20018 San Sebastián, Spain*
[4] *Fritz-Haber-Institut der Max-Planck-Gesellschaft, Berlin, Germany*
[5] *University of Vienna, Faculty of Physics, Strudlhofgasse 4, A-1090, Vienna, Austria*

(Dated: submitted to Phys. Rev. Lett., November 29, 2011)

Ab initio calculations of the loss-function of potassium intercalated and electron loaded bundles of single walled carbon nanotubes yield a channeled charge carrier plasmon, without perpendicular dispersion. Experimentally, we probe the momentum dependent loss-function of nano-wires consisting of only a few potassium intercalated single walled carbon nanotubes by angle resolved electron energy loss spectroscopy and confirm this intrinsic channeling. The charge carrier plasmon energy is via *in-situ* intercalation tunable in the near visible infrared energy range from 0.85 eV to 1.15 eV.

PACS numbers: 73.20.Mf,73.22.-f,78.20.Bh

In conventional bulk metallic systems the collective electronic excitations spectrum is comprised of free charge carrier or intra-band plasmons and inter-band plasmons. Plasmons are, in analogy to sound waves, longitudinal density fluctuations that propagate through the electron plasma. In the optical limit at vanishing momenta $q = \hbar\, k \rightarrow 0$ the metallic intra-band plasmon scales with the electron density n_e and occurs at $\omega_P^2 = n_e\, e^2/m^\star\, \varepsilon_0$. Staged graphite intercalation compounds (GIC) are a special case of metallic systems with well defined stoichiometry. The intra-band plasmon as well as the inter-band plasmon of the electronic π and σ bands in GIC are long known [1].

Another important classification of plasmons is the distinction of bulk and surface modes. The latter are confined to the interface of two dielectric media where the sign of the frequency dependent dielectric response $\varepsilon(\omega)$ flips. For a Drude metal in vacuum the free surface plasmon is found at $\omega_S = \omega_P/\sqrt{2}$. In a free charge carrier plasma there is a quadratic dispersion relation [2], whereas the intra- and inter-band plasmon dispersion of actual solids is influenced by the band structure. [3, 4] The two dimensional domain of a surface plasmon cancels any defined momentum state or dispersion relation in the perpendicular direction. Well defined momentum states only apply in the surface.

Individual single walled carbon nanotubes (SWNT) or thin wires of them are archetypes of quantum wires with unique and strongly anisotropic dielectric properties, and macroscopic aligned films of them [5–7] may be envisaged as a nano-meshed meta-material. In dielectric meta-materials the plasmon response may be further inflicted by crystal local field effects (LFE). These are of more pronounced importance in isolated sheets or even nano-wires. [8–11] The full electronic excitation spectrum beyond the optical limit is accessible by electron energy loss-spectroscopy (EELS). [7] Angle resolved EELS (AR-EELS) assesses plasmon energies and dispersion relations. [12, 13]

The present work addresses the frequency and momentum dependent dielectric response of freestanding metallic nano-wires. Our *ab initio* calculations on K intercalated and electron loaded SWNT bundles show a channeled low energy charge carrier plasmon. The electron density and hence the frequency of the charge carrier plasmon in freestanding SWNTs is tuned by *in situ* potassium intercalation. We confirm a channeled and tuneable charge carrier plasmon in the near infrared region from 0.85 eV to 1.15 eV by AR-EELS measurements.

Density functional theory (DFT) calculations for bulk SWNT bundles were performed using the real-space projector augmented wave (PAW) code GPAW [14], with the PBE exchange-correlation (xc)-functional [15]. The optimized unit cells for bundles of (10,10)/(17,0) SWNTs of 2.470/4.272 Å in the axial direction and 16.95/16.88 Å between SWNTs in the bundle cross section were employed, containing 40/68 carbon atoms and 2 potassium atoms, respectively. Atomic coordinates were relaxed until forces were below 0.05 eV/Å. Charged calculations with $Q = -1, -2, \ldots, -8$ e/cell were performed with a uniform background potential to eliminate interactions between neighboring unit cells. To determine the affect of lattice expansion due to charging of the SWNT bundles, calculations for the highest considered electron loading e/C = 12.5% were performed expanding the lattice parameters in the bundle cross section by $1\%, 2\%, \ldots, 10\%$. Even the 10 % lattice expansion of the SWNT bundle did not noticeable affect the charge carrier plasmon energy.

A Monkhorst-Pack k-point sampling with 25/15 k-points along the axial direction, and 4×4 k-points in the bundle cross section yields a momentum transfer resolution $\Delta\mathbf{q}$ of ≈ 0.1 Å^{-1}. Loss function calculations were performed using linear response time dependent DFT within the random-phase approximation [16], with LFEs included.

Samples for AR-EELS are freestanding films of vertically aligned SWNT, that were prepared as described in Ref. [17] The individual nano-wires are composed of typically 5 to 7 SWNT and are arranged in a sparse random array with a bulk density as low as $\rho \approx 0.05$ g cm^{-3}. [18, 19] The diameters of the individual SWNT are ~ 2 nm. Commercial potassium getters from SAESgetters were used to evaporate potassium and perform successive *in situ* intercalation of the nano-wires. The angle resolved loss function of the potassium intercalated carbon nano-wires was measured in a purpose built EELS spectrometer [20], operated at an energy and momentum resolution of 80 meV and 0.03 Å^{-1}. The incident beam is in normal transmission parallel to the net-alignment, and the momentum transfer q is predominantly perpendicular to the axis of the nano-wires.

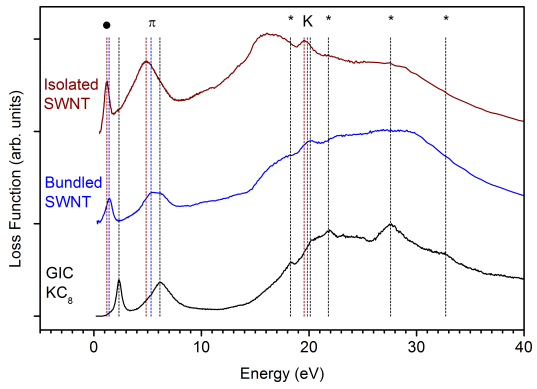

FIG. 1: (Color online) The loss-functions of fully n-doped allotropes of sp^2 carbon networks. The loss-functions were recorded at a momentum transfer $q = 0.1$ Å^{-1}. Vertical lines compare the positions of plasmon modes in the three different samples. • denotes the charge carrier plasmon, K the atomic $K_{3p} \rightarrow K_{4s}$ transition, π the inter-band plasmon of the electronic π system, and $\star$ the multiple oscillators of the $\pi + \sigma$ electrons.

The loss-function of GIC KC_8, fully intercalated bulk SWNT, and the fully intercalated sparse nano-wires are shown in Fig. 1. All three potassium intercalated allotropes of sp^2 carbon exhibit a charge carrier plasmon at small energies (•), an inter-band excitation of the electronic π system at intermediate energies (π), and lastly a more structured $\pi+\sigma$ inter-band response of the remaining C_{2p} electronic system ($\star$). The atomic $K_{3p} \rightarrow K_{4s}$ excitation (K) is found embedded in the $\pi + \sigma$ structures. The most apparent observation is that all charge carrier and inter-band plasmons are downshifted when going from KC_8 via bulk bundles of SWNTs, to sparse nano-wires. This behavior is entirely conceivable within the Drude-Lorentz model, where the longitudinal plasma frequency ω_L is offset to the transversal (optical) plasma frequency ω_T according to $\omega_L^2 = \omega_T^2 + \omega_P^2$. The smaller density results in a lower ω_P. The additional electrons are provided by potassium counter-ions whose, atomic concentration are derived from the C_{1s} and K_{2p} core level excitations shown in Fig. 4. The different densities, observed peak positions and widths of the intra-band plasmon at the individual doping steps are collected in Table I.

TABLE I: Potassium concentrations and intra-band plasmon for carbon nano-wires in comparison to that of fully intercalated bundled SWNTs and KC_8 from Ref. [21]. The subscripts $_B$ and $_S$ denote bulk and surface plasmons.

Step	K/C(%)	$\rho(g\,cm^{-3})$	E(eV)	ε_∞	$\Gamma(eV)$
prist.	-	~ 0.05	-	1	-
I	1.6	~ 0.05	0.85_S	1	0.5
II	5.5	~ 0.05	1.05_S	1	0.5
III	8.4	~ 0.05	1.10_S	1	0.5
IV	12.5	~ 0.05	1.15_S	1	0.5
bundled	12.5	1.3	1.4_B	6.1	0.7
GIC KC_8	12.5	2.3	2.4_B	6.7	0.2

The changes in the loss-function during successive potassium intercalation of the nano-wires are shown in Fig. 2. The vertical dashed line marks the unchanged position of the π plasmon. The intra-band plasmon (•) is gradually upshifted with increasing potassium concentrations. The square of the plasmon position ω_P^2 is plotted against the potassium concentration in the right panel of Fig. 2. Our current studies on the nano-wires are compared to pioneering studies on graphite intercalation compounds [1] as well as preceding studies on bundled SWNTs [21]. All three sp^2 carbon systems exhibit a monotone increase of ω_P^2 with increasing K/C ratio. A key difference here is the sharp onset of a intra-band plasmon near a K/C of 4-5% in bundled SWNTs as opposed to the smooth behavior in the nano-wires. In bundled SWNT the intra-band plasmon occurs only when the semiconducting SWNTs are driven metallic, too [22]. We suggest that the competition for charge transfer only works for interstitial channels inside a mixed bundles. Neither the calculated all metallic or semiconducting bundles nor the surface dominated nano-wires provide such channels.

The empirical data on bundles and nano-wires in the right panel of Fig. 2 is clearly beyond the classical homogenous Drude model, that would feature a straight line. In contrast, the calculated charge carrier plasmon in electron loaded all (10,10) or (17,0) bundles lies close to the interpolated data from intercalated graphite. It also scales linearly with the charge transfer.

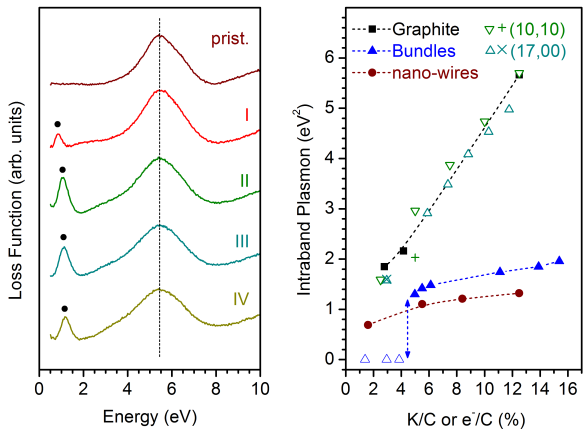

FIG. 2: (Color online) Left panel: Low energy range of the loss functions of successively potassium intercalated carbon nano-wires. Right panel: Square of the peak position of the charge carrier plasmon versus potassium concentration for graphite (squares), bundled SWNTs (up triangles), isolated SWNTs (circles) in comparison to calculations on electron loaded (open down and up triangles) and K intercalated (+, ×) all (10,10) and all (17,0) bundles, respectively. Dotted lines are guides for the eye.

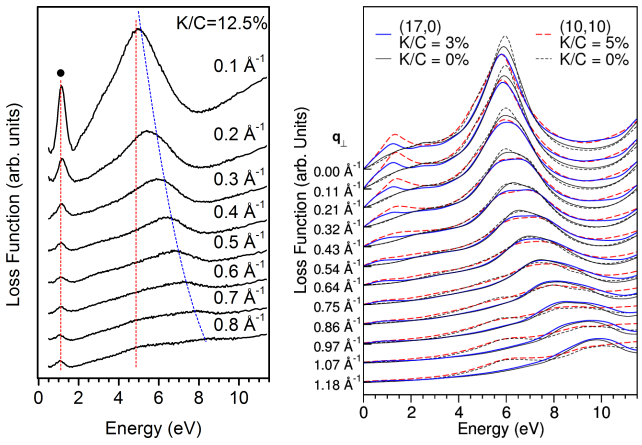

FIG. 3: (Color online) *left panel:* AR-EELS of K intercalated carbon nanotubes. The momentum transfer q is perpendicular to the net-alignment. *right panel:* Calculated loss-function of pristine and K intercalated bulk bundles for $q_\perp$.

The comparison of electron loaded and potassium intercalated calculations suggests that there is a complete charge transfer in GIC as well as K intercalated semiconducting SWNT, but only a fractional ($\sim 2/3$) charge transfer in K intercalated metallic SWNT. The very different changes of the π resonance of the C1s core edges in Fig. 4 of KC_8 and K intercalated nano-wires underpins this possibility. On this basis, we propose that on the nano-wires K ions will first occupy the fully coordinated sites and only later lower coordinated sites with reduced partial charge transfers. Thus the increase in ω_P^2 levels off, and its energy is finely tuned by the K concentration.

Regarding the different plasmon energies in nano-wires and bulk bundles, the nano-wires resemble the textbook example of a meta-material consisting of parallel metallic cylinders. The key characteristics of such a classical system [23] with a material intrinsic ω_P but only a very low filling ratio $f \ll 1$ are: (i) a bulk on-axis plasmon that scales with the filling ratio $f \cdot \omega_P$, and (ii) an orthogonal localized surface plasmon at $\omega_P/\sqrt{1+\varepsilon_\infty}$. In the present case of negligible dielectric screening ε_∞ becomes unity and the surface plasmon arises at $\omega_P/\sqrt{2}$. The low filling ratio of $f \approx 0.07$ switches off the on-axis plasmon, but the orthogonal surface mode is preserved.

In this intuitive model we can interpret the down scaled intra band plasmon in nano-wires as a localized surface mode of the charge carrier plasmon in bulk bundles. The scaling of the curves in Fig. 2 yields a scaling factor of $\omega_{pB}^2/\omega_{pS}^2$ of $\sim$ 4/3 for carbon nano-wires.

The momentum dispersion of the loss-function in the left panel of Fig. 3 reveals the elementary electronic excitation spectrum beyond the optical limit ($q \to 0$). The dotted verticals and traces highlight the dispersion of individual features. We find a pair of one non-dispersing and one dispersive plasmon for the π inter-band plasmon [11]. The charge carrier plasmon is observed exclusively as a non-dispersing mode. The calculations of the loss-functions in the right panel of Fig. 3 were performed for pristine and K intercalated bundles. The low energy range shown here features the π-plasmon as well as a new charge carrier plasmon above 1 eV specific to intercalated bundles. Calculations for $q_\parallel$ are shown in Fig. 4. Here the additional charge carrier response shows a dispersive behavior for the lowest momentum transfers before it is quickly dampened by interband transitions. The comparison of $q_\parallel$ and $q_\perp$ reveals the exclusive appearance of the non-dispersive π plasmon for $q_\parallel$ in (17,0) and $q_\perp$ in (10,10). The non dispersive π plasmon is therefore always found for q along armchair direction.[24]. The charge carrier plasmon in K intercalated armchair and zigzag bundles is found to be independent of q along armchair or zigzag but utterly different for $q_\parallel$ and $q_\perp$.

While the charge carrier plasmon behaves ordinarily for $q_\parallel$, the gradual damping and absence of orthogonal dispersion with $q_\perp$ are unexpected in a bulk system. They are the hallmark of one-dimensional channeling on individual SWNT *inside* a bulk bundle.

As counterintuitive this *ab initio* finding might seem, it is fully corroborated by no less unexpected experimental findings [21]. The current AR-EELS experiments demonstrate a doping dependent and non $q_\perp$ dispersing intraband plasmon in carbon-nanowires. The *ab initio* calculations on intercalated and electron loaded bundles provide an *ab initio* footing for the interpretation of the observed plasmon as the charge carrier response in SWNT and also explain why there could no dispersive charge carrier plasmon have been found in earlier AR-EELS studies

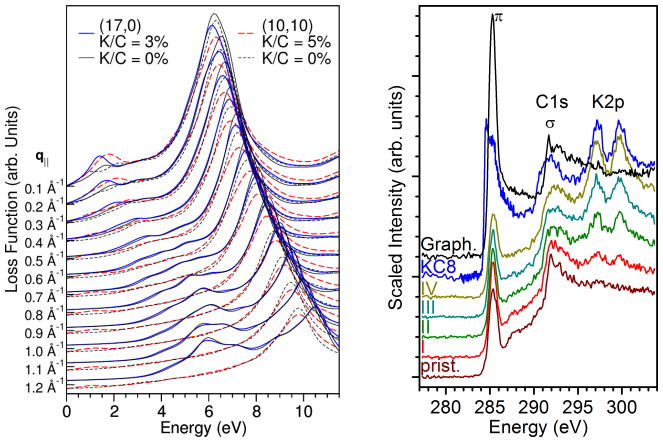

FIG. 4: (Color online) *left panel:* Calculated loss-function of pristine and K intercalated bulk bundles for $q_{\|}$. *right panel:* Core level loss edges of the C_{1s} and K_{2p} in graphite, KC_8, doped and pristine carbon nanowires.

on K intercalated bulk bundles of SWNTs [21].

Another very important aspect of one-dimensional electronic systems is the electronic Tomonaga liquid [25]. It was first evidenced on mixed SWNT material by the characteristic power law onset in photoemission spectra [26]. It was believed that the 2/3 of semiconducting SWNTs act as spacers to maintain one-dimensional metallic channels inside the bulk bundles. Later, it was discovered that bulk bundles of all metallic SWNTs are a Tomanaga liquid, too. [27] The latter surprising finding is fully in-line with our notion that metallic SWNTs in a bundle do act as independent channels. The channeling of the intra-band plasmon is not only provided by the nano-wires morphology but it is indeed an intrinsic property of each and every SWNT.

Summarizing, we have demonstrated the direct experimental access to the full spectrum of localized and delocalized inter band and charge carrier plasmons on carbon nano-wires and put fractional charge transfer in alkali intercalated bundles of SWNT as well as the intrinsic nature of channeled charge carrier plasmons in SWNT on an *ab-initio* footing. The intrinsic local channeling gives rise to uniform and well defined bulk properties, *independent* of the detailed morphology. This robustness against variations in the micro-scale is a versatile aspect for plasmonic devices based on carbon nanotubes.

We acknowledge funding by DFG PI 440/4, European Research Council Advanced Grant DYNamo (ERC-2010-AdG -Proposal No. 267374), Spanish MICINN (FIS2010-21282-C02-01), "Grupos Consolidados UPV/EHU del Gobierno Vasco" (IT-319-07), ACI-Promociona (ACI2009-1036) and European Community e-I3 ETSF project (Contract No. 211956). CK acknowledges an APART fellowship 11456 of the Austrian Academy of Science. DJM acknowledges funding through the Spanish "Juan de la Cireva" program (JCI-2010-08156).

[1] J. J. Ritsko, E. J. Mele, and I. P. Gates, Phys. Rev. B **24**, 6114 (1981).
[2] J. Lindhard, Kgl. Dans. Videsk. Selsk. Mat. Fys. Medd. **28**, 1 (1954).
[3] P. Nozieres and D. Pines, Phys. Rev. **113**, 1254 (1959).
[4] H. Ehrenreich and M. H. Cohen, Phys. Rev. **1**, 786 (1959).
[5] Y. Murakami, S. Chiashi, Y. Miyauchi, M. H. Hu, M. Ogura, T. Okubo, and S. Maruyama, Chem. Phys. Lett. **385**, 298 (2004).
[6] Y. Murakami, E. Einarsson, T. Edamura, and S. Maruyama, Phys. Rev. Lett. **94**, 087402 (2005).
[7] O. Stéphan, D. Taverna, M. Kociak, K. Suenaga, L. Henrard, and C. Colliex, Phys. Rev. B **66**, 155422 (2002).
[8] S. L. Adler, Phys. Rev. **126**, 413 (1962).
[9] N. Wiser, Phys. Rev. **1**, 62 (1963).
[10] G. Onida, L. Reining, and A. Rubio, Rev. Mod. Phys. **74**, 601 (2002).
[11] C. Kramberger, R. Hambach, C. Giorgetti, M. H. Rummeli, M. Knupfer, J. Fink, B. Buchner, L. Reining, E. Einarsson, S. Maruyama, et al., Phys. Rev. Lett. **100**, 196803 (2008).
[12] T. Pichler, M. Knupfer, M. S. Golden, J. Fink, A. Rinzler, and R. E. Smalley, Phys. Rev. Lett. **80**, 4729 (1998).
[13] M. Knupfer, T. Pichler, M. S. Golden, J. Fink, A. Rinzler, and R. E. Smalley, Carbon **37**, 733 (1999).
[14] J. Enkovaara, C. Rostgaard, J. J. Mortensen, J. Chen, M. Dułak, L. Ferrighi, J. Gavnholt, C. Glinsvad, V. Haikola, H. A. Hansen, et al., J. Phys.: Condens. Matter **22**, 253202 (2010).
[15] J. P. Perdew, K. Burke, and M. Ernzerhof, Phys. Rev. Lett. **77**, 3865 (1996).
[16] J. Yan, J. J. Mortensen, K. W. Jacobsen, and K. S. Thygesen, Phys. Rev. B **83**, 245122 (2011).
[17] Y. Murakami and S. Maruyama, Chem. Phys. Lett. **422**, 575 (2006).
[18] H. M. Duong, E. Einarsson, J. Okawa, R. Xiang, and S. Maruyama, Jpn. J. Appl. Phys. **47(4)**, 1994 (2008).
[19] E. Einarsson, H. Shiozawa, C. Kramberger, M. H. Rummeli, A. Gruneis, T. Pichler, and S. Maruyama, J. Phys. Chem. C **111**, 17861 (2007).
[20] J. Fink, Adv. Elec. & Elec. Phys. **75**, 121 (1989).
[21] X. Liu, T. Pichler, M. Knupfer, and J. Fink, Phys. Rev. B **67**, 125403 (2003).
[22] C. Kramberger, H. Rauf, M. Knupfer, H. Shiozawa, D. Batchelor, A. Rubio, H. Kataura, and T. Pichler, Phys. Rev. B **79**, 195442 (2009).
[23] T. McNeish, G. Gumbs, and A. Balassis, Phys. Rev. B **77**, 235440 (2008).
[24] S. Dmitrović, T. Vuković, B. Nikolić, M. Damnjanović, and I. Milošević, Phys. Rev. B **77**, 245415 (2008).
[25] S. Tomonaga, Prg. of Theo. Phys. **5**, 544 (1950).
[26] H. Ishii, H. Kataura, H. Shiozawa, H. Yoshioka, H. Otsubo, Y. Takayama, T. Miyahara, S. Suzuki, Y. Achiba, M. Nakatake, et al., Nature **426**, 540 (2003).
[27] P. Ayala, Y. Miyata, K. De Blauwe, H. Shiozawa, Y. Feng, K. Yanagi, C. Kramberger, S. R. P. Silva, R. Follath, H. Kataura, et al., Phys. Rev. B **80**, 205427 (2009).